



Effects of the Removal of 0.1 μm Particles in Industrial Cleanrooms with a Fan Dry Coil Unit (FDCU) Return System

Ti Lin¹, Yun-Chun Tung², Shih-Cheng Hu^{1*}, Chen-Yen Lin¹

¹ Department of Energy and Refrigerating Air-Conditioning Engineering, National Taipei University of Technology, 1, Sec. 3, Chung-Hsiao E. Rd., Taipei City 106, Taiwan (R.O.C.)

² Department of Industrial Education, National Taiwan Normal University, 162, Sec. 1, He-ping E. Rd., Taipei City 106, Taiwan (R.O.C.)

ABSTRACT

A wall-return ventilation system, containing ceiling-supply and wall-return air grilles, is traditionally used in non-unidirectional airflow cleanrooms. In such a wall-return cleanroom, the pathways of return airflow towards the wall-return grilles may be affected by locations and layouts of the production lines and tool equipment; moreover, especially considering the needs for relocation of production lines and rearrangement of tool equipment in the industrial cleanrooms, this study proposed a fan dry coil unit (FDCU) return system, containing ceiling-supply and ceiling-return air grilles, and conducted experimental works in a full-scale cleanroom to investigate the performance of the innovative and traditional ventilation systems. The influences of air change rates and supply air plenum pressures on the removal of 0.1 μm particles were examined in the experiment. Results presented in this paper were subject to the particle size of 0.1 μm . The FDCU-return ventilation arrangement may provide viable solutions to effective contamination control. The results showed that the innovative FDCU-return system can effectively eliminate about 50% of 0.1 μm particles from the cleanrooms more than the conventional wall-return system. Moreover, the outcomes from this study suggested that particle removal rates for the given cleanrooms were significantly affected by air change rates.

Keywords: Cleanroom; FDCU (a fan dry coil unit); Particle; Ventilation.

INTRODUCTION

An air recirculation system of a raised-floor return ventilation arrangement has been employed to industrial cleanrooms and received increased attention (Hu *et al.*, 1996; Fu *et al.*, 2001; Hu *et al.*, 2002a, 2002b; Hu and Chuah, 2003; Hu and Wu, 2003; Hu and Hsiao, 2005; Hu and Chen, 2007; Hu *et al.*, 2009). In such raised-floor return air system, the clean air is introduced from ceiling grilles and then extracted from the raised perforated floor. In order to maintain unidirectional airflow, enough plenums of supply and return air are required to the cleanrooms with better cleanliness class, and cause the increase of construction cost. However, a wall-return ventilation arrangement has been employed to the air recirculation system for non-unidirectional cleanrooms, and reduced the cost of construction due to without the return air plenum. In a traditional arrangement of the airflow pathway in the

cleanrooms, shown in Fig. 1, the supply air (SA) is introduced from ceiling air grilles and the return air (RA) is extracted from the wall air grilles close to and vertical to the floors. In such a wall-return cleanroom, the directions of airflows could be largely consistent with the movements of gravitationally settling particles in industrial cleanrooms or those of gravitationally settling bio-aerosols in bio-cleanrooms, such as pharmaceutical cleanrooms and hospital operating rooms, while the return air shafts (RASs) are normally required. Electric power demand for fan filter units (FFUs) can be increased due to long airflow paths of airflows in the recirculation systems (i.e., from the FFUs outlets through the RASs, then back to the inlets of FFUs). In addition, the airflow distribution can be significantly influenced by the locations of production tools and devices as well as by the movements of operators. In summary, the wall-return system results in the following problems: (1) FFUs must have sufficient external static pressure to overcome the resistance of the return-air grilles (RAGs), RASs, and dry cooling coils (DCCs), (2) the downward cold supply air toward to the wall grilles encounters the upward hot air currents from the process tools, and (3) the positions of the RASs and DCCs are not changeable.

Kato *et al.* (1992) indicated that changes in the arrangements

* Corresponding author. Tel.: 886-2-27712171, ext. 3512;
Fax: 886-2-27314949
E-mail address: fl0870@ntut.edu.tw

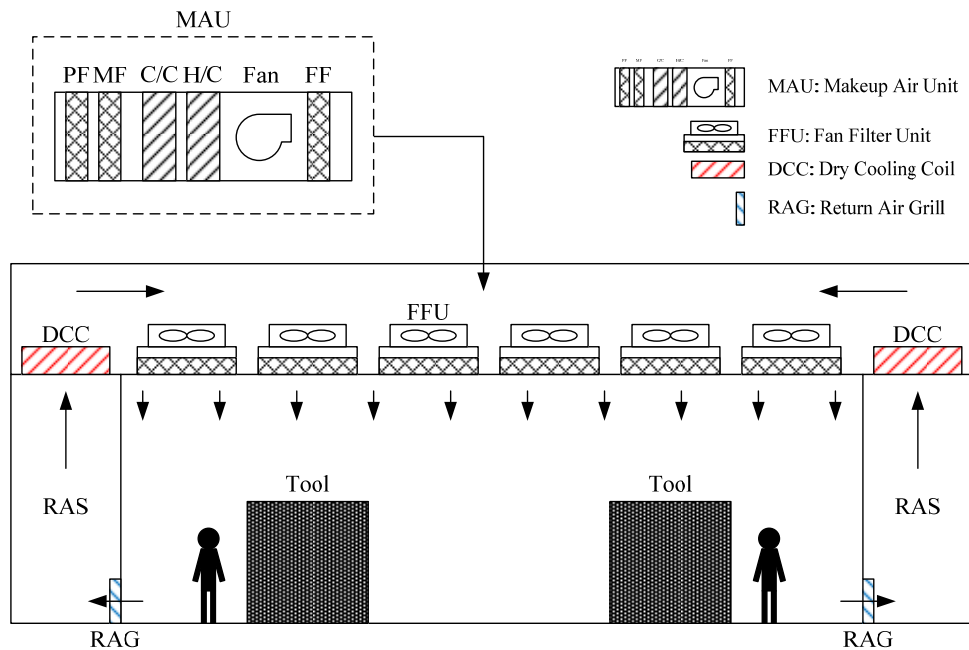


Fig. 1. A traditional wall-return ventilation cleanroom.

or in the numbers of exhaust openings have no significant effect on the entire flow fields. However, such changes often have great influence on the particle diffusion fields (for $0.3\ \mu\text{m}$ particles), since the particle transportation path is changed by the position of the exhaust outlets. Murakami *et al.* (1989) reported that a locally balanced supply-exhaust airflow system (the supply and exhaust airflow rates balanced locally within a flow unit) exhibits better particle removal efficiency than a wall-return cleanroom. Yang *et al.* (2009) employed numerical modeling using the Re-Normalization Group (RNG) $k\text{-}\epsilon$ method to examine the effects of various ventilation designs for an ISO Class 5 cleanroom on contaminant dispersion and particle concentrations. They identified the optimal ventilation options confirmed by experimental measurements. Shimada *et al.* (1996) experimentally and theoretically studied the change in concentration distribution of particulate contaminants emitted in a room in order to investigate whether the transport of contaminants in a room with a source of particles can be predicted by numerical simulation. Their results also indicated that the contaminants introduced near the room floor diffuse more than predicted. However, the calculated concentrations agreed almost quantitatively with the measured results, except near the floor and walls. Hu and Tung (2002) used Eulerian and Lagrangian methods to examine the airflow fields and particle fates in non-unidirectional-flow cleanrooms, and have found that a wall-return type cleanroom is less effective in dispatching particles to return/exhaust exits than the locally balanced supply-return airflow rate system (i.e., the exhaust grilles are installed so that the supply and exhaust airflow rates are balanced locally in that space). They also found that

particles generated close to return grilles are more effectively returned from the cleanroom. Zhao and Wu (2005) used computational fluid dynamics (CFD) to investigate particle diffusion with gravitational sedimentation in a clean room with different ventilation modes. The results showed that the ventilation mode, particle source location, and air exchange rate can influence particle distribution in a clean room.

In industrial buildings, cleanrooms designed with the ceiling-return arrangement normally present fewer barriers compared with the wall-return arrangements, especially considering the needs for relocation of production lines and layouts of the production tools in such facilities. With the increasing application and advancement of FFUs for air recirculation in cleanrooms (Chen *et al.*, 2007; Xu *et al.*, 2007), installing supply and return air grilles on the ceiling has become feasible. Such arrangements applied the characteristics of negative pressure within supply-air plenums to facilitate the return of air from the interior of the cleanroom to the ceiling grilles. Lu and Howarth (1996) used a numerical model to predict the movements of air and aerosol particles in two interconnected ventilated zones. The particle deposition and migration are mainly influenced by the particle properties, the ventilation conditions, and the airflow patterns in the two zones. Particles migrate faster with a high ventilation rate. Larger particles ($4\ \mu\text{m}$) deposit much faster than smaller particles ($2\ \mu\text{m}$). Additionally, sub-micron particles have a great impact on the product yields in semiconductor cleanrooms (Hu and Wu, 2003), and they have very small terminal velocity when moving in cleanrooms (Hinds, 1999). For industrial cleanrooms with high heat dissipation, such as semiconductor cleanrooms for IC testing and thin filming (with furnaces), the cleanliness level and room air temperature must be maintained and controlled within a

strict range, and due to the advances in semiconductor manufacturing technology, the sizes of the particles of concern currently fall into the sub-micron regions. Therefore, the present study has focused on the concentration variation of $0.1\ \mu\text{m}$ particles in industrial cleanrooms. However, it was noted that particles larger than $100\ \mu\text{m}$ in diameter will not be removed effectively using any of the ventilation schemes (Tung *et al.*, 2010). This is because gravitational forces are dominant—making it difficult to remove the large particles from cleanrooms. For removing $10\ \mu\text{m}$ -diameter particles from the empty cleanroom, three ventilation models exhibited similar efficiency to those of submicron particles; whereas all the ventilation models become essentially ineffective to remove when the tool coverage ratios are above 38%. The arrangements of locally balanced ceiling-return, wall-return, and four-way ceiling-return ventilation models can effectively remove particles of 1, 0.1, and $0.01\ \mu\text{m}$ in diameters for the tool coverage ratios of 60%, 38%, and 0%, respectively.

In order to solve the above-mentioned problems in the wall-return ventilation system, this paper proposes a unique local air distribution scheme to maintain the cleanliness level within requirements and to effectively remove the dissipated heat. Fig. 2 shows the new proposed the ventilation system of fan dry coil units (FDCUs) in which the supply and return grilles were installed on the ceiling and the dissipated heat was removed by the FDCUs located just above the process tools. Fig. 3 demonstrates the schematic diagram of the FDCU. In order to identify and develop viable solutions for effective contamination control in critical industrial buildings, this study aimed to experimentally examine and compare the performance of the traditional and innovative ventilation arrangements in a full-scale cleanroom with a typical IC testing machine, that emits particles and heat.

METHODS

A full-scale cleanroom of $4.8\ \text{m}$ (length) \times $6.3\ \text{m}$ (width) \times $2.8\ \text{m}$ (height) in the X, Y, and Z directions was set up and maintained at $23 \pm 0.5\ ^\circ\text{CDB}$ and $16 \pm 0.5\ ^\circ\text{CDP}$ in the experiments. Two dummy tools, each size of $1.6\ \text{m}$ (length) \times $1.2\ \text{m}$ (width) \times $2.4\ \text{m}$ (height), and a process tool of $0.6\ \text{m}$ (length) \times $0.9\ \text{m}$ (width) \times $1\ \text{m}$ (height), a semiconductor testing machine, were located in the cleanroom. Figs. 4 and 5 show the layouts of the cleanroom with the FDCU-return and the wall-return ventilation arrangements. The arrangements of return air in each room model were different in location and individual grille sizes, while those of supply air grilles (SAGs) were the same. The SAGs consisted of 12 FFUs (each with size of $1200\ \text{mm}$ -length \times $600\ \text{mm}$ -width \times $275\ \text{mm}$ -height). Ultra low penetration air (ULPA) filters were installed with the FFUs; hence, the measured background particle concentrations in the cleanrooms were zero particle/ m^3 . Three sets of FDCUs (each size of $1200\ \text{mm}$ -length \times $600\ \text{mm}$ -width \times $455\ \text{mm}$ -height) on the ceiling were arranged in the FDCU-return cleanroom to catch the rising air streams toward the ceiling exit. Six sets of RAGs (each sizing $1200\ \text{mm} \times 300\ \text{mm}$), located on the opposite walls near the floor and corners, were installed in the wall-return cleanroom. The six RAGs were sealed by plates and all control valves of DCCs were closed when experimental work was conducted in the FDCU-return cleanroom. Three FDCUs were sealed by plates and turned off, when experimental work was conducted in the wall-return cleanroom.

The process tool was located under one of FFUs, as shown in Fig. 5. Particles and heat were released from an outlet of the process tool. The area, air velocity, and air temperature of the outlet were $0.57\ \text{m}^2$, $4.6\ \text{m/s}$, and 37°C , respectively. An ultrasonic vibrator, located by the process tool, was provided to generate polystyrene latex spheres

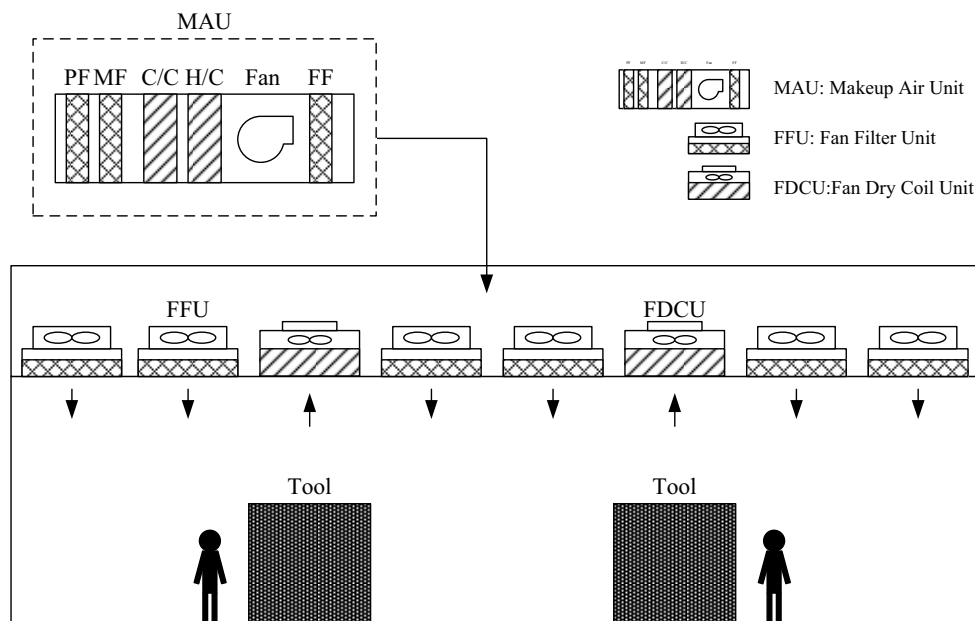


Fig. 2. An innovative FDCU-return ventilation cleanroom.

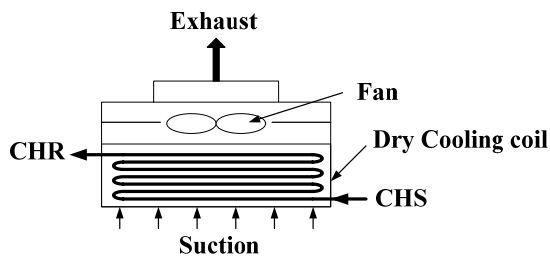


Fig. 3. Schematic of FDCU (CHS: chilled water supply, CHR: chilled water return).

(PSLs), more than 92% of which were 0.1 μm -diameter particles. In order to simulate the emission of contaminants from the process tool, PSLs from the vibrator were drawn into the process tool and then emitted from the outlet of the process tool. The source concentrations of PSL at the outlet of the process tool ranged from approximately 10,400,000–12,700,000 particles/ m^3 . A diluter was linked to the inlet of a He-Ne laser particle counter (Met one 2100, with accuracy and sampling airflow rate of $\pm 10\%$ and 1.7

m^3/h ($1 \text{ ft}^3/\text{m}$), respectively) to measure the high particle concentrations from the process tool. The laser particle counter was also linked to a manifold with multi-channel to measure the particle concentrations at 14 sampling points. Table 1 lists the locations of each sampling point in the cleanroom. The pressures in the supply air plenum (SAP) were set at +2, -10, and -20 Pa by the frequency converters of the FDCUs in the FDCU-return system, respectively. The supply air velocity from FFUs were set at 0.22, 0.31, and 0.38 m/s by the 5-speed controllers of the FFUs respectively, and they referred to as a setting of Channel 4, 2, and 1 (or CH 4, 2, and 1), respectively. The cleanroom was maintained at a positive pressure of +12 Pa by a frequency converter of a makeup air unit (MAU). In order to minimize the measurement error of particle concentration, resulted from the uncertainty of outdoor air, high efficiency particulate air (HEPA) filters were installed at the end of the supply air duct of the MAU. In the present study, the measured concentration of particles (particles/ ft^3) was normalized by that of the particle source (particles/ ft^3), generated from the process tool.

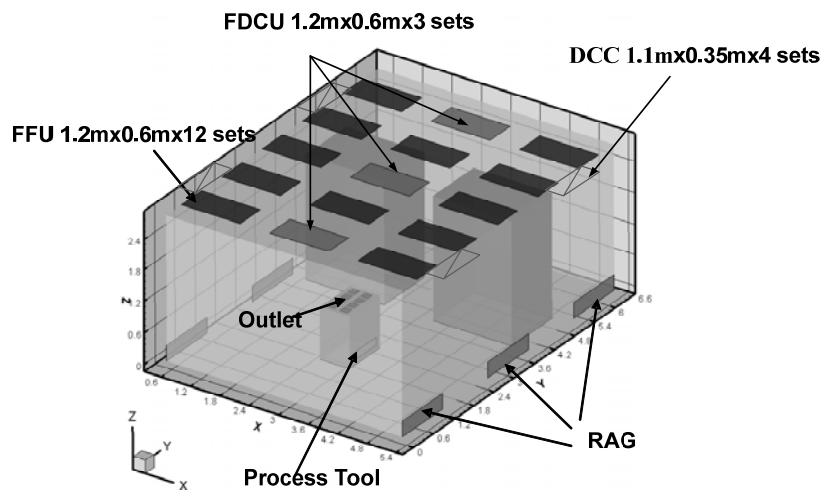


Fig. 4. Configuration of a cleanroom with wall-return and FDCU-return arrangements.

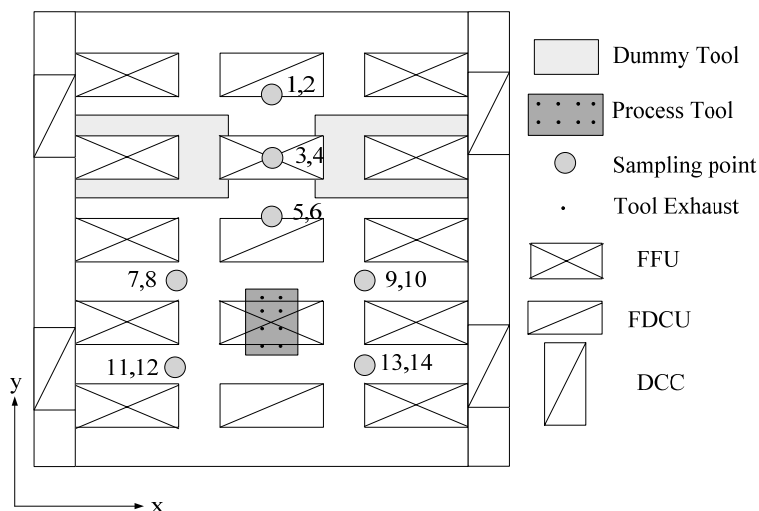


Fig. 5. Plan of a cleanroom with wall-return and FDCU-return arrangements.

Table 1. Coordinates of sampling points in the cleanroom.

Sampling point	X (m)	Y (m)	Z (m)
1	2.9	5.85	1.5
2	2.9	5.85	1.2
3	2.9	4.2	1.5
4	2.9	4.2	1.2
5	2.9	3.45	1.5
6	2.9	3.45	1.2
7	1.7	2.5	1.5
8	1.7	2.5	1.2
9	1.7	1.3	1.5
10	1.7	1.3	1.2
11	4.1	2.5	1.5
12	4.1	2.5	1.2
13	4.1	1.3	1.5
14	4.1	1.3	1.2

MEASUREMENT UNCERTAINTY

In the present study, a standard deviation (SD) refers to the spread of the experimental data and the variability in the measures. An error bar along with a mean value (a plotted symbol) designates a range of one standard deviation on one measurement, and visually compares two quantities. Five replications of experimental measurement were conducted to get the mean and standard deviation of the concentration of PSLs for each sampling point. The standard deviation, a descriptive error bar, is the typical or average difference between the data points and their mean (Cunning et al., 2007). The equation for standard deviations is as follows:

$$SD = \sqrt{\frac{\sum(X - \bar{X})^2}{n - 1}} \tag{1}$$

where X represents an individual data point, \bar{X} the mean value of data points, and n the number of data points.

Moreover, when dealing with given independent variables, each of which is characterized by a degree of uncertainty, error propagation is adopted as a way of determining the degree of uncertainty in a function of these variables. The formulas for determining uncertainty of the measured or output quantity Y (represented as standard deviations in this study) are presented as follows:

Addition and subtraction: $Y = X1 + X2$ or $Y = X1 - X2$

$$\Delta Y = \sqrt{(\Delta X1)^2 + (\Delta X2)^2} \tag{2}$$

Multiplication and division: $Y = X1 \times X2$ or $Y = X1/X2$

$$\Delta Y = Y \sqrt{\left(\frac{\Delta X1}{X1}\right)^2 + \left(\frac{\Delta X2}{X2}\right)^2} \tag{3}$$

here, $X1$ and $X2$ refer to the measured quantities with their uncertainties, $\Delta X1$ and $\Delta X2$, determined by standard deviations; Y refers to a new quantity called the measurand, determined from other quantities $X1$ and $X2$; and ΔY is the uncertainty of the measurand.

RESULTS AND DISCUSSION

Effects of Air change Rates and Ventilation Arrangements

Fig. 6 shows the influence of air changes per hour (ACH) on the averaged normalized concentrations of PSLs (hereafter referred to particles) in the cleanrooms with ventilation arrangements of the wall-return and FDCU-return types. The averaged normalized concentrations of

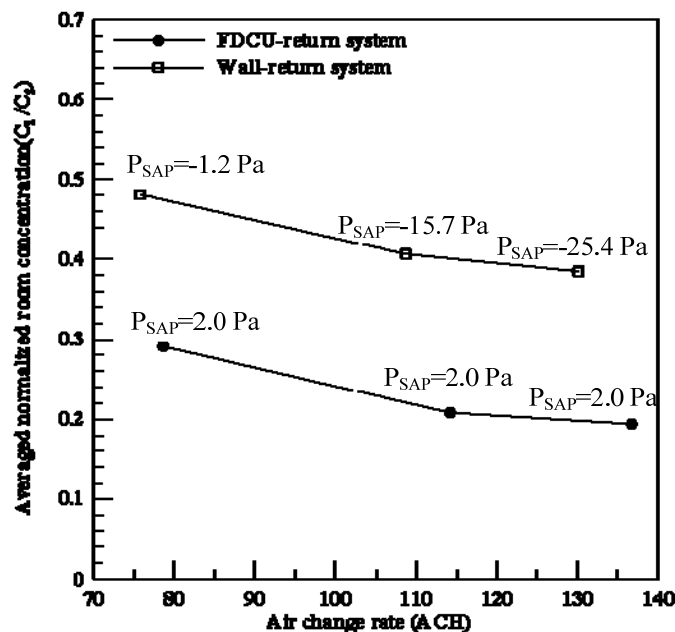


Fig. 6. Averaged normalized room concentrations of particles.

particles in the wall-return cleanroom ranged from 0.39 to 0.48 at 72–127 ACH, whereas the concentrations in the FDCU-return cleanroom ranged from 0.17 to 0.33 at 70–139 ACH. It was observed that increasing the ACH helped reduce the average particle concentrations in both the wall-return and FDCU-return cleanrooms. An increase of about 1.8 times the 72 ACH in the wall-return cleanroom reduced the averaged particle concentrations by about 19%, while that of about 2 times the 70 ACH in the FDCU-return cleanroom reduced the average particle concentrations by about 52%. The FDCU-return ventilation system,

therefore, exhibited a greater benefit in reducing the averaged particle concentrations in the cleanroom by about 31 to 59% over the wall-return ventilation system.

Fig. 7 indicates that the normalized concentrations at 14 sampling points in the FDCU-return cleanroom were lower than the ones in the wall-return cleanroom. Fig. 5 reveals that points 1–4 were far from the process tool, whereas points 1 and 2 were located behind the dummy tools and the furthest from the process tool, and points 3 and 4 were located between the dummy tools. Accordingly, the concentration levels at points 1 and 2 were the lowest, and

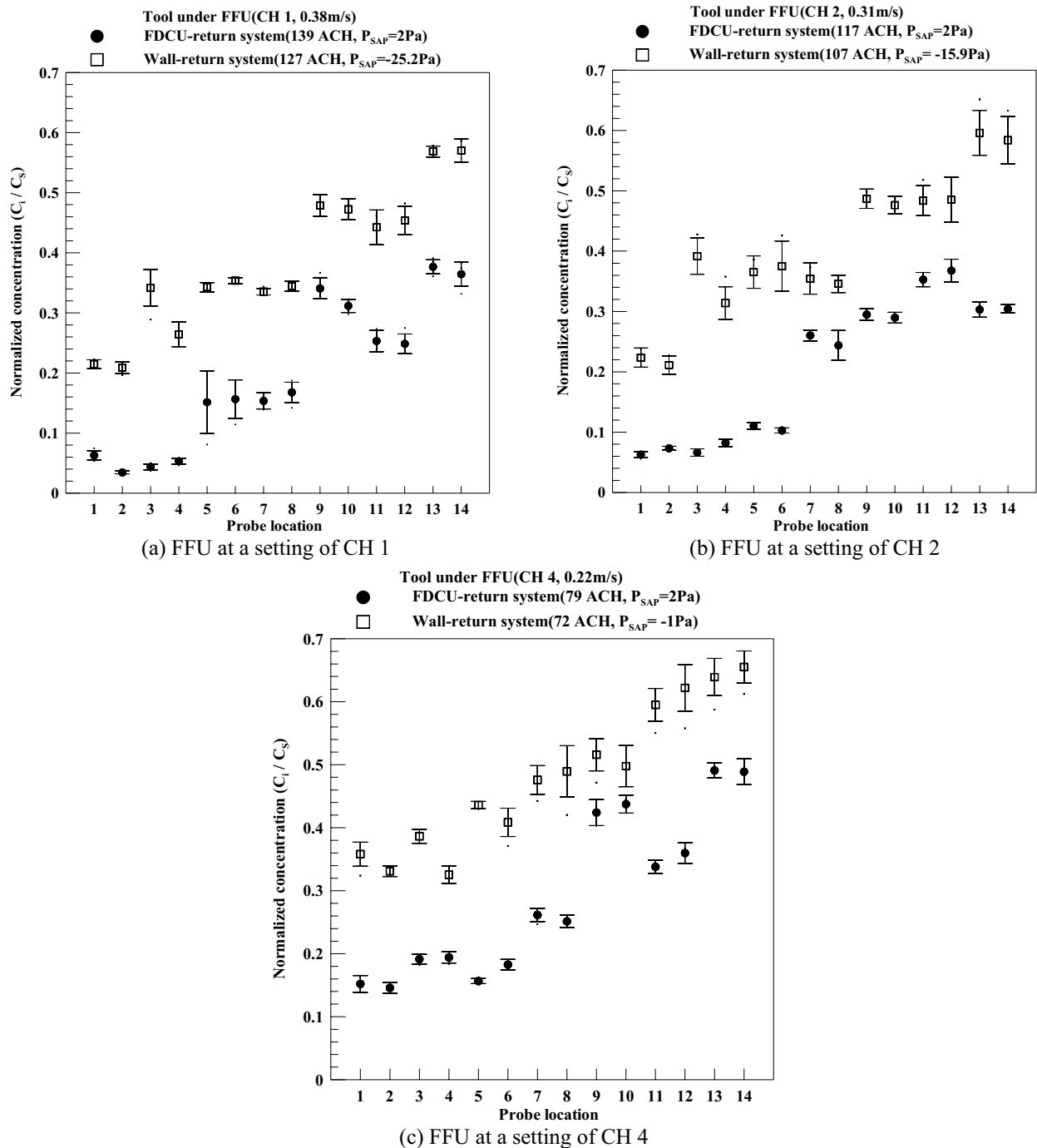


Fig. 7. Profiles of normalized particle concentrations.

those at points 3 and 4 were moderately high since recirculation zones were expectedly formed between the dummy tools. The measured particle concentrations at points 11–14 were higher than those at other points, because points 11–14 were located by the process tool and easily contaminated by the particles from the process tool.

Effects of ACH and SAP Pressures in the FDCU-return Cleanroom

For FDCU-return cleanrooms, the recirculation airflow was driven by the combination of FFUs and FDCUs, and the pressures in the SAP may be either positive or negative, affected by the FFUs and FDCUs. For wall-return cleanrooms, the recirculation airflow was driven only by FFUs, and the SAP characterized a negative pressure, due to its location of the inlet of FFUs. Moreover, in order to prevent the ingress of contaminants, industrial cleanrooms were designed with positive pressure relative to its neighbor rooms or areas (e.g., SAP and RASs). Hence, the pressures in the SAP were less than that in the cleanroom (i.e., +12 Pa) and were controlled at +2, -10, and -20 Pa, respectively, corresponding to the settings of CH 1, 2, and 4 at the FFUs.

This study examined how the SAP pressures influenced the particle concentrations in the FDCU-return cleanrooms. As shown in Fig. 8, the pressures in the SAP had insignificant impact on the averaged concentrations of particles in the FDCU-return cleanrooms, but higher settings of FFU speed resulted in lower average concentrations of particles in the room. However, higher negative pressures in the SAP (e.g., -20 Pa) at each setting of FFUs speed increased the possibility of the infiltration of particles into the SAP, and caused higher averaged room concentrations of particles, which were insignificant nevertheless, because the ULPA filters of FFUs arrested

most particles from the SAP into the cleanrooms. Moreover, the pressure changes in the SAP affected the air change rates in the cleanrooms, since the system's combination of FFUs and FDCUs and their airflow pathways increased the airflow resistance of the recirculation air system. This resistance caused a reduction in ACH. Fig. 9 reveals the normalized room concentrations of particles at 14 sampling points at different SAP pressures, corresponding to three settings of FFU speed. The increase in the SAP pressure resulted from the increase in the airflow rates of the FDCUs. The normalized room concentrations of particles at points 1–4 and 11–14 were low and high levels, respectively. The ACH and the pressures in the SAP affected the particle concentrations at each sampling point.

In the case of the process tool under the FFU, Table 2 summarizes all the measured results of ACH, SAP pressures, and averaged normalized room particle concentrations at three settings of FFUs speed and two arrangements of return-air system. Compared with the wall-return system, at the same setting of FFUs speed, the FDCU-return system can reach a higher air change rate due to a shorter airflow pathway and a smaller airflow resistance. When the process tool was located under the FFU in the wall-return cleanrooms, the upward hot air from the process tool will encounter the downward supply air of FFUs and then spread to the entire room in the wall-return cleanroom. On the contrary, in the FDCU-return cleanroom, the upward hot air will be exhausted by the FDCUs located next to the FFUs.

CONCLUSIONS

This study qualitatively and quantitatively investigated the influences of ventilation arrangements, ACH, and SAP

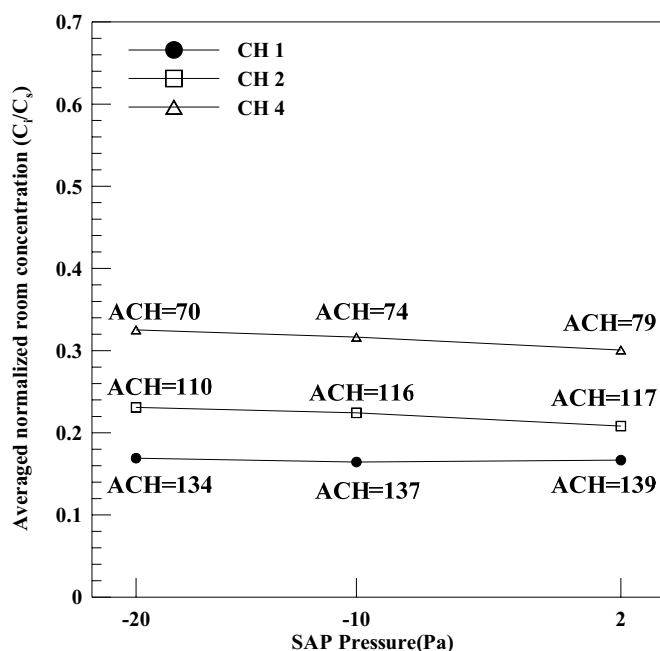
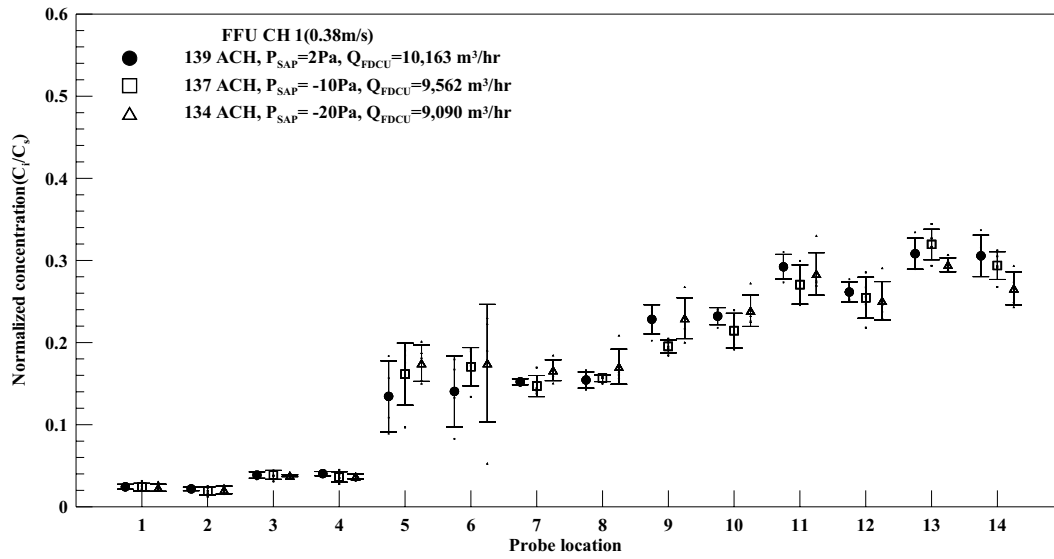
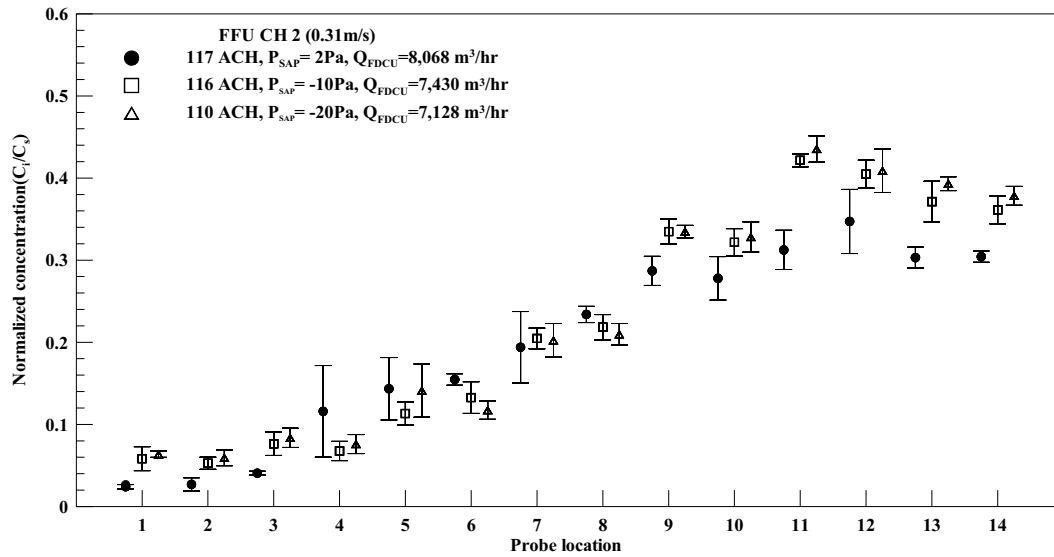


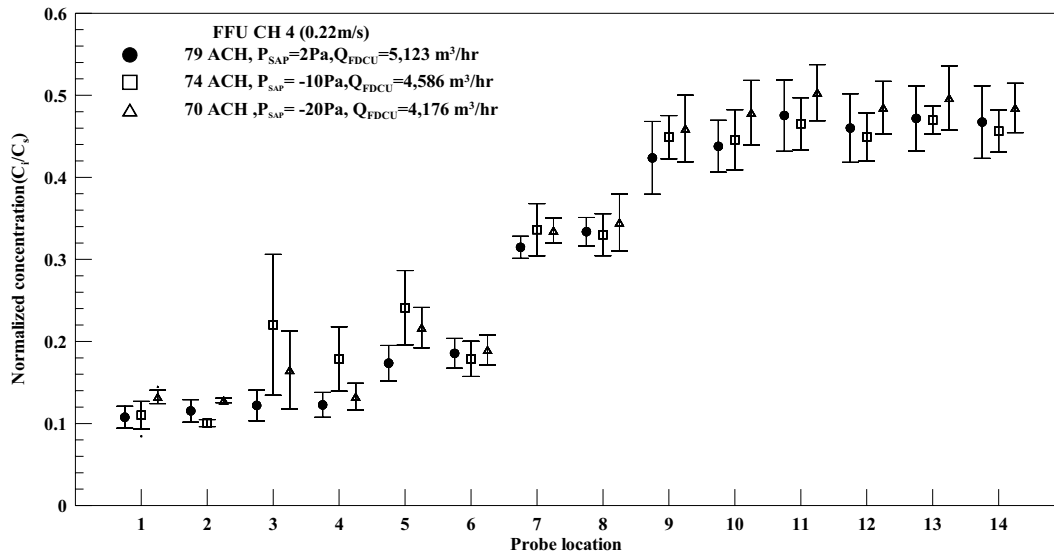
Fig. 8. Averaged normalized concentrations of particles in the FDCU-return cleanroom.



(a) FFU at a setting of CH 1



(b) FFU at a setting of CH 2



(c) FFU at a setting of CH 4

Fig. 9. Profiles of normalized particle concentrations in the FDCU-return cleanroom.

Table 2. Averaged normalized room concentrations of particles at three settings of FFUs speed.

Cleanroom type	FFU air velocity (m/s) ¹	P _{SAP} (Pa)	ACH	C _{room,averaged} /C _{tool,emitting}
<i>FFUs speed set at CH 1</i>				
FDCU-return	0.38	2.0	139	0.17
FDCU-return	0.37	-10.0	137	0.16
FDCU-return	0.37	-20.0	134	0.17
Wall-return	0.35	-25.2	127	0.39
<i>FFUs speed set at CH 2</i>				
FDCU-return	0.32	2.0	117	0.20
FDCU-return	0.32	-10.0	116	0.22
FDCU-return	0.30	-20.0	110	0.23
Wall-return	0.29	-15.9	107	0.41
<i>FFUs speed set at CH 4</i>				
FDCU-return	0.22	2.0	79	0.30
FDCU-return	0.20	-10.0	74	0.32
FDCU-return	0.19	-20.0	70	0.33
Wall-return	0.20	-1.0	72	0.48

Note 1: the air velocity of each FFU was measured at a distance of 0.15 m from its outlet, and was averaged by eight different measured points.

pressures on the removal of 0.1 μm particles. The ventilation arrangements of wall-return and FDCU-return were used to maintain contamination control for non-unidirectional airflow cleanrooms with air change rates ranging from 70 to 139 ACH, recommended for ISO cleanliness class 6 (ISO, 2001). Results indicate that the FDCU-return system has a greater benefit in particle removal than the wall-return system. The air change rate dominates the average concentrations of particles in the cleanrooms, while the influence of the SAP pressures on the averaged concentrations of particles may be ignored in the FDCU-return cleanrooms. The effect of increasing ACH on the particle removal in the FDCU-return cleanroom is obviously better than that in the wall-return cleanroom. Moreover, in order to have the best efficiency of removing particles from the industrial cleanrooms, it is suggested that the arrangement of the FDCU-return ventilation system be considered. It is noted that the results presented in this paper are subject to the particle size of 0.1 μm . Future researches may like to expand the particle sizes larger or smaller than 0.1 μm .

ACKNOWLEDGMENTS

The authors would like to thank the National Science Council of Taiwan for financially supporting this research under contract number 98-ET-E-0027-001-ET.

REFERENCES

- Chen, J.J., Lan, C.H., Jeng, M.S. and Xu, T. (2007). The Development of Fan Filter Unit with Flow Rate Feedback Control in a Cleanroom. *Build. Environ.* 42: 3556–61.
- Cumming, G., Fidler, F. and Vaux, D.L. (2007). Error Bars in Experimental Biology. *J. Cell Biol.* 177: 7–11.
- Fu, W.S., Chen, S.F., and Yang, S.J. (2001). Numerical Simulation of Effects of Moving Operator on the Removal of Particles in Clean Room. *Aerosol Air Qual. Res.* 1: 37–45.
- Hinds, W.C. (1999). *Aerosol Technology*, 2nd ed, New York, John Wiley & Sons, Inc.
- Hu, S.C., Wu, Y.Y. and Liu, C.J. (1996). Measurements of Air Flow Characteristics in a Full-scale Clean Room. *Build. Environ.* 31: 119–128.
- Hu, S.C., Chuah, Y.K. and Huang, S.C. (2002). Performance Comparison of Axial Fan and Fan-filter Unit Type Clean Rooms by CFD. *ASHRAE Trans.* AC-02-17-4.
- Hu, S.C., Chuah, Y.K. and Yen, M.C. (2002). Design and Evaluation of a Mini-environment for Semiconductor Manufacture Processes. *Build. Environ.* 37: 201–208.
- Hu, S.C. and Tung, Y.C. (2002). Performance Assessment for Locally Balanced and Wall-return Turbulent Clean Rooms by the Stochastic Particle Tracking Model. *Int. J. Archit. Sci.* 3: 146–162.
- Hu, S.C. and Chuah, Y.K. (2003). Deterministic Simulation and Assessment of Air Recirculation Performance of Unidirectional Flow Cleanrooms That Incorporate Age of Air Concept. *Build. Environ.* 38: 563–570.
- Hu, S.C. and Wu, T.M. (2003). Experimental Studies of Airflow and Particle Characteristics of a 300 mm POUP/LPU Minienvironment System. *IEEE Trans. Semicond. Manuf.* 16: 660–667.
- Hu, S.C. and Hsiao, T.R. (2005). Particle Dynamics in a Front Opening Unified Port/Load Port Unit Minienvironment in the Presence of a 300 mm Wafer in Various Positions. *Aerosol Sci. Technol.* 39: 185–195.
- Hu, S.C. and Chen, C.C. (2007). Locating the Very Early Smoke Detector Apparatus (VSDA) in Vertical Laminar Cleanrooms According to the Trajectories of Smoke Particles. *Build. Environ.* 42: 366–371.
- Hu, S.C., Ku, C.W., Shih, Y.C., and Hsu, K. (2009). Dynamic Analysis on Particle Concentration Induced by

- Opening the Door of a Front Opening Unified Pod (FOUP) that Loaded with 25 Pieces of 300 mm Wafer Manufacturing Processes. *Aerosol Air Qual. Res.* 9: 139–148.
- International Organization for Standardization (ISO, 2001). *ISO 14644-4, Cleanrooms and Associate Controlled Environments-Part 4 Design, Construction, and Start-up*. The Institute of Environmental Sciences and Technology (IEST), IL, USA.
- Kato, S., Murakami, S. and Nagano, S. (1992). Numerical Study on Diffusion in a Room with a Locally Balanced Supply-Exhaust Air Flow Rate System. *ASHRAE Trans.* 98: 218–238.
- Lu, W. and Howarth, A.T. (1996). Numerical Analysis of Indoor Aerosol Particle Deposition and Distribution in Two-zone Ventilation System. *Build. Environ.* 31: 41–50.
- Murakami, S., Kato, S. and Suyama, Y. (1989). Numerical Study on Diffusion Field as Affected by Arrangement of Supply and Exhaust Openings in Conventional Flow Type Clean Room. *ASHRAE Trans.* 95: 113–127.
- Shimada, M., Okuyama, K., Okazaki, S., Asai, T., Matsukura, M. and Ishizu, Y. (1996). Numerical Simulation and Experiment on the Transport of Fine Particles in a Ventilated Room. *Aerosol Sci. Technol.* 25: 242–255.
- Tung, Y.C., Hu, S.C., Xu, T. and Wang, R.H. (2010). Influence of Ventilation Arrangements on Particle Removal in Industrial Cleanrooms with Various Tool Coverage. *Build. Simul.* 3: 3–13.
- Xu, T., Lan, C.H. and Jeng, M.S. (2007). Performance of Large Fan-filter Units for Cleanroom Applications. *Build. Environ.* 42: 2299–2304.
- Yang, C., Yang, X., Xu, T., Sun, L. and Gong, W. (2009). Optimization of Bathroom Ventilation Design for an ISO Class 5 Clean Ward. *Build. Simul.* 2: 133–142.
- Zhao, B. and Wu, J. (2005). Numerical Investigation of Particle Diffusion in a Clean Room. *Indoor Built Environ.* 14: 469–479.

Received for review, March 7, 2010

Accepted, August 12, 2010